NASA TN D-1766

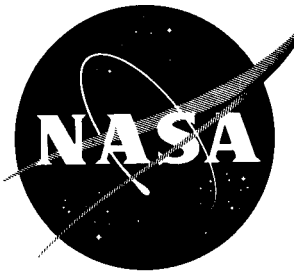

TECHNICAL NOTE

D-1766

WIND-TUNNEL TESTS OF TWO VTOL

PROPELLERS IN DESCENT

By Paul F. Yaggy and Kenneth W. Mort

Ames Research Center
Moffett Field, Calif.

NATIONAL AERONAUTICS AND SPACE ADMINISTRATION

WASHINGTON

March 1963

NATIONAL AERONAUTICS AND SPACE ADMINISTRATION

TECHNICAL NOTE D-1766

WIND-TUNNEL TESTS OF TWO VTOL PROPELLERS IN DESCENT

By Paul F. Yaggy and Kenneth W. Mort

SUMMARY

The vertical or near-vertical descent of propeller-driven, VTOL aircraft causes the propellers to experience negative inflow angles. As the rate of descent is increased from zero, the propeller passes through the turbulent vortex-ring state. Tests of a rigid and a flapping propeller were made at various rates of descent from 0 to 6,000 feet per minute to determine the effects of operation in the vortex-ring state upon the thrust force produced by the propellers. The tests covered a disc loading range from 0 to 36 pounds per square foot.

The results of these tests showed that thrust oscillations as large as ±75 percent of the steady-state thrust occurred, and that the average period of the oscillations was about 0.2 second, apparently independent of other test parameters.

INTRODUCTION

Vertical or near-vertical descent of VTOL-type, propeller-driven aircraft subjects the propellers to operation at negative inflow angles. As the descent velocity is increased, the propeller passes from the normal operating state into the less stable vortex-ring state. Operation in this less stable state gives rise to oscillating shaft forces on the propeller (see, e.g., ref. 1).

Tests of two propellers were made in the Ames 40- by 80-Foot Wind Tunnel to investigate the effects of descent rate on the shaft thrust force. The propellers selected for these tests provided a disc-loading range from 0 to 36 pounds per square foot. They were tested at tunnel airspeeds equivalent to rates of descent from 0 to 6,000 feet per minute. Although reference 1 showed that the oscillating thrust forces were accompanied by oscillating torque, oscillating in-plane forces, and oscillating out-of-plane moments, no attempt was made to measure the values of these parameters in the present investigation.

NOTATION

A	propeller disc area, sq ft
b	propeller blade chord, ft
C_{L_d}	propeller blade-section design lift coefficient, $\frac{\text{section design lift}}{q_l b}$
C_T	thrust coefficient, $\frac{T}{\rho n^2 D^4}$
D	propeller diameter, ft
h	propeller blade thickness, ft
J	propeller advance ratio, $\frac{V_\infty}{nD}$
n	propeller rotational speed, rps
r	radial distance to any propeller blade section
q_l	local dynamic pressure at any propeller blade section, lb/ft^2
R	propeller blade tip radius
T	thrust, lb
V_∞	free-stream velocity, fps
V_d	rate of vertical descent, fpm
X	dimensionless radial location of any propeller blade section, r/R
α	geometric angle of attack of the thrust axis to the free stream, deg
β	propeller blade angle measured at the 0.7-radius station, deg
ΔC_T	maximum amplitude of the oscillating thrust coefficient
ρ	mass density of air, slugs/cu ft

MODEL AND APPARATUS

Propellers

The propellers selected for the investigation were greatly different in design. One was of conventional rigid design, and the other was an articulated (flapping out of plane only) propeller designed to eliminate shaft out-of-plane

moments. The physical characteristics of the propellers are listed in the following table:

Propeller	No. 1 Vertol 76	No. 2 Curtiss C634S-C500
Diameter	9.5 ft	12.0 ft
No. of blades	3	3
Blade construction	Wood and steel	Hollow steel
Airfoil section	NACA 0009	NACA 16 Series
Blade designation	Q76R1002	858-7C4-36
Activity factor/blade	178	150
Flapping hinge offset	3 in.	---
Blade plan-form curves for the two propellers are presented in figure 1.		

Testing Apparatus

For the tests, the propellers were mounted on the propeller test stand in the Ames 40- by 80-Foot Wind Tunnel as shown in figure 2. The shroud or wind fairing was isolated from the tunnel balance system so that only propeller forces and moments were measured. To simulate the descent condition, the propellers were mounted with the thrusting face directed downstream rather than in the conventional manner.

Instrumentation

Strain-gaged beams were attached to the test stand in such a manner as to be deformed when the stand deflected under thrust loading. The beams were calibrated and the data recorded dynamically on a recording oscillograph. Both steady-state and oscillating loads were then obtained by analysis of the wave forms appearing on the oscillograph records.

Tests

The propellers were tested under the following conditions:

	Rigid propeller	Flapping propeller
1. Rotational speed, rpm	700 to 1100	700 to 1410
2. Velocity along the flight path, fpm	0 to 6000	0 to 3000
3. Angle of attack of the propeller axis to the flight path, deg	180	120 to 180

At each test condition, the blade angle of the propeller was varied to obtain the effects of varying disc loading.

Reduction of Data

The data obtained during the tests were steady-state thrust measurements from the wind-tunnel balance and dynamic thrust measurements from the strain-gaged beams on the support struts. Values of both the average thrust and the amplitude of the oscillating thrust were obtained from the dynamic measurements. The average values agreed well with the wind-tunnel balance measurements. The values of steady-state and oscillating thrust were reduced to coefficient form and are presented as functions of the propeller advance ratio.

RESULTS AND DISCUSSION

The steady-state thrust coefficient for the two propellers is shown as a function of propeller advance ratio in figures 3 and 4. The curve shapes reflect the transition of the propellers through the various working states as advance ratio is decreased. The transition proceeds from the normal-propeller state through the vortex-ring state toward the windmill-brake state. The loss in thrust during the turbulent vortex-ring state is clearly indicated. The amount of thrust loss is seen to vary with thrust-axis angle of attack. This variation is due to the sweeping away of the vortex ring by the crossflow on the propeller.

The oscillation of the thrust in the region of the vortex-ring state is demonstrated in figures 5 and 6. The envelope of the oscillation is shown superposed on the variation of the steady-state thrust coefficient. It is seen that oscillations as large as ±75 percent of the steady-state thrust occurred. The period of oscillation was about 0.2±0.03 second for all the conditions represented and appeared to be independent of the test parameters.

The significance of the thrust oscillations in terms of operating characteristics is more clearly seen when the oscillating thrust is considered as a percentage of the steady-state thrust at various disc loadings and rates of descent. Such variations were calculated from the data in figures 5 and 6 using 12-foot diameter and 1117 rpm for the rigid propeller, and 9.5-foot diameter and 1410 rpm for the flapping propeller. The results are shown in figure 7 for the flapping propeller at several angles of attack, and in figure 8 for the rigid propeller at 180° angle of attack. In each case, the descent velocity is the true-vertical rate of descent.

From figures 7 and 8 it is seen that, for a given rate of descent, the thrust oscillation generally diminishes as disc loading is increased. This trend is observed until maximum thrust oscillation occurs. Beyond this condition, the behavior varies depending upon the angle of attack. Further, for a given disc loading, it is seen that the thrust oscillation increases in magnitude with rate of descent as the propeller moves into the vortex-ring state. Then, with further increase in the rate of descent the oscillation decreases as the propeller moves toward the windmill-brake state.

Ames Research Center
National Aeronautics and Space Administration
Moffett Field, Calif., Dec. 19, 1962

REFERENCE

1. McLemore, H. Clyde, and Canon, Michael D.: Aerodynamic Investigation of a Four-Blade Propeller Operating Through an Angle-of-Attack Range From 0° to 180°. NACA TN 3228, 1954.

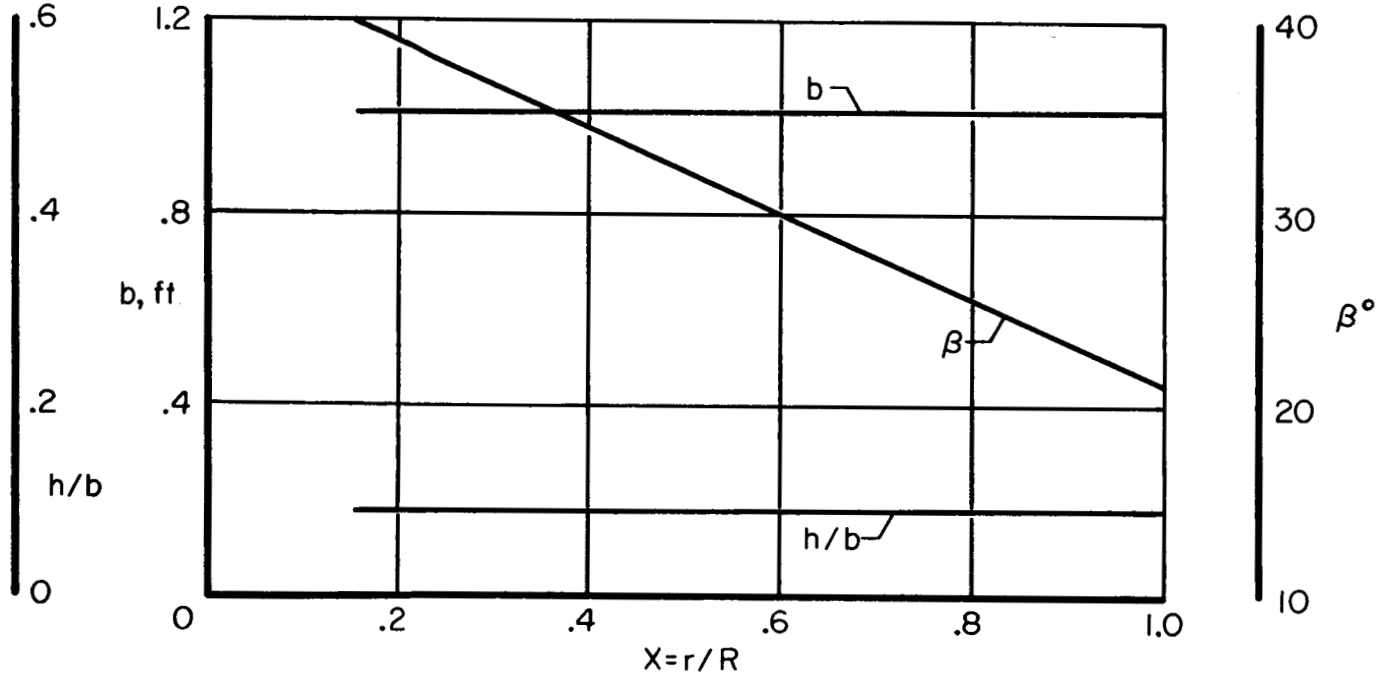

(a) Flapping propeller.

Figure 1.- Blade plan-form curves.

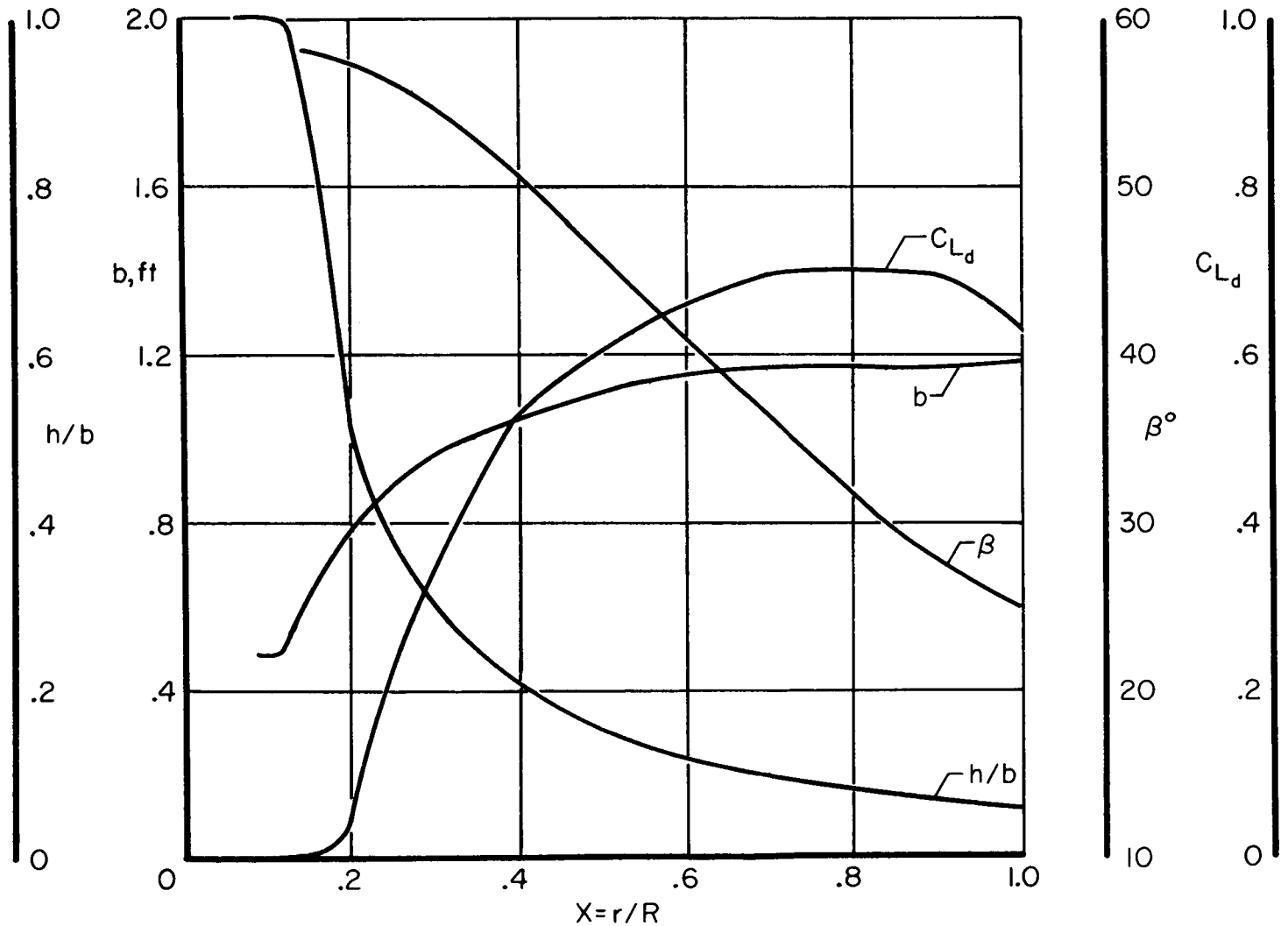

(b) Rigid propeller.

Figure 1.- Concluded.

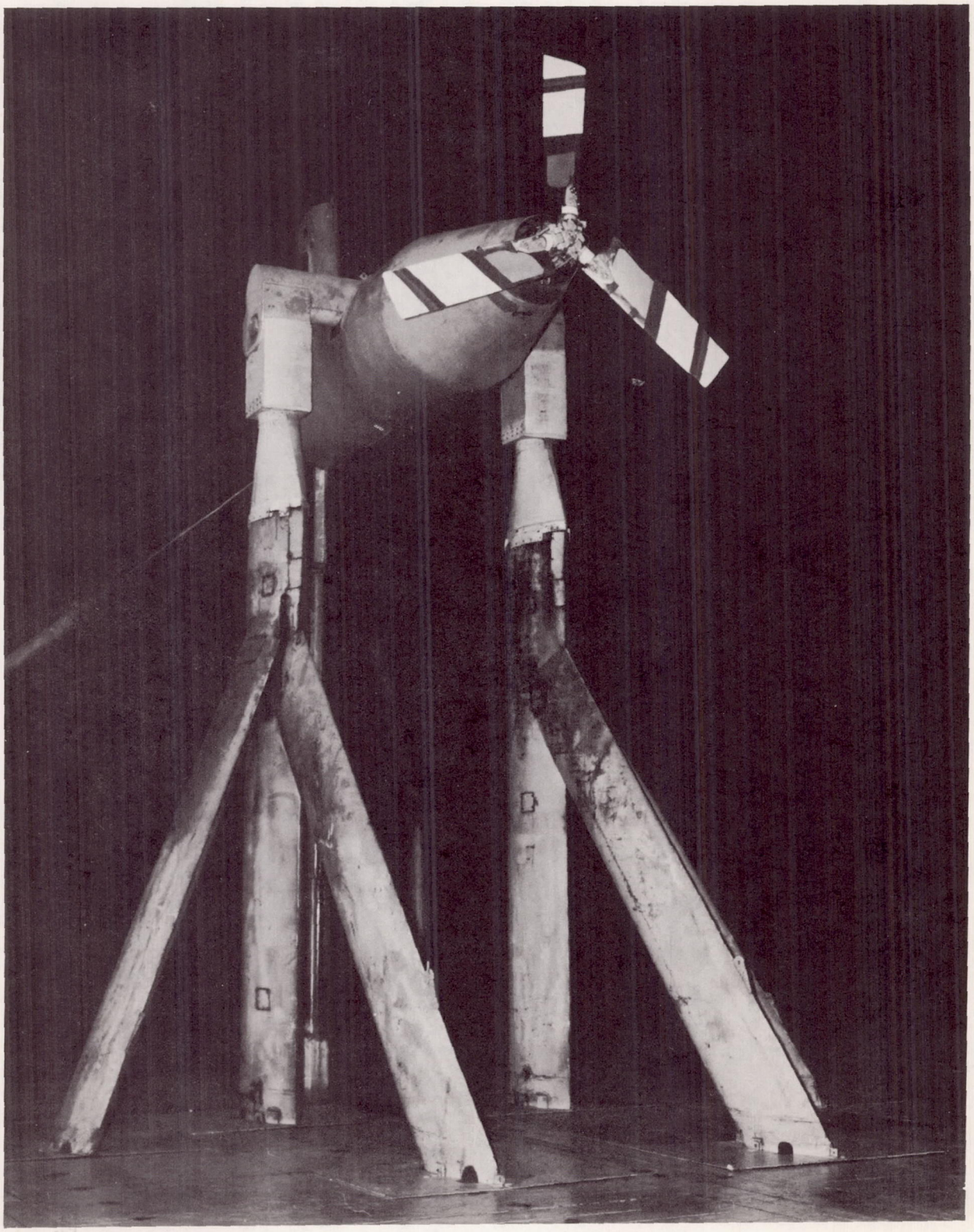

A-25877

Figure 2.- The flapping propeller mounted in the Ames 40- by 80-Foot Wind Tunnel.

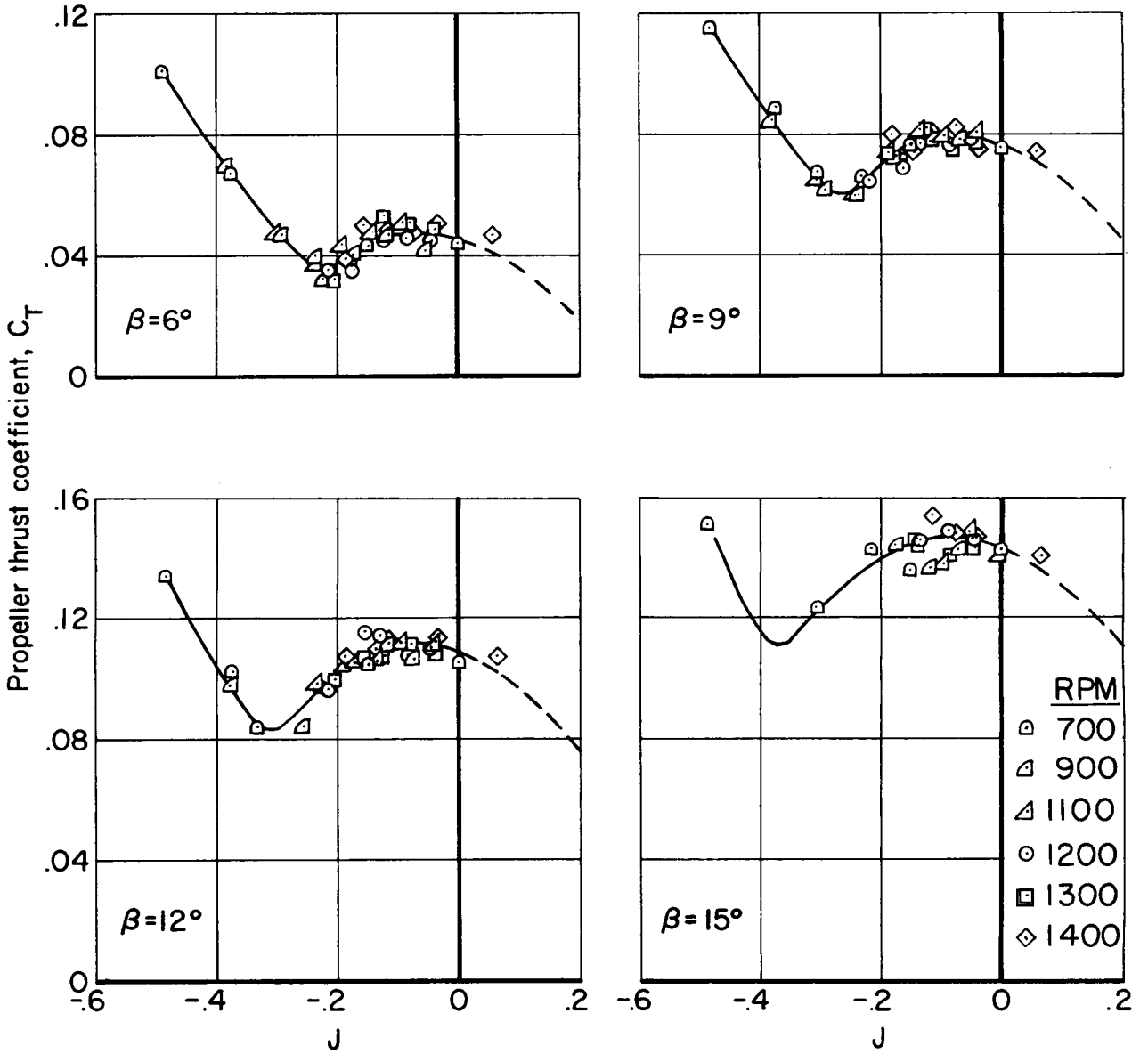

(a) $\alpha = 180^{\circ}$

Figure 3.- Steady-state thrust coefficient as a function of propeller advance ratio for the flapping propeller.

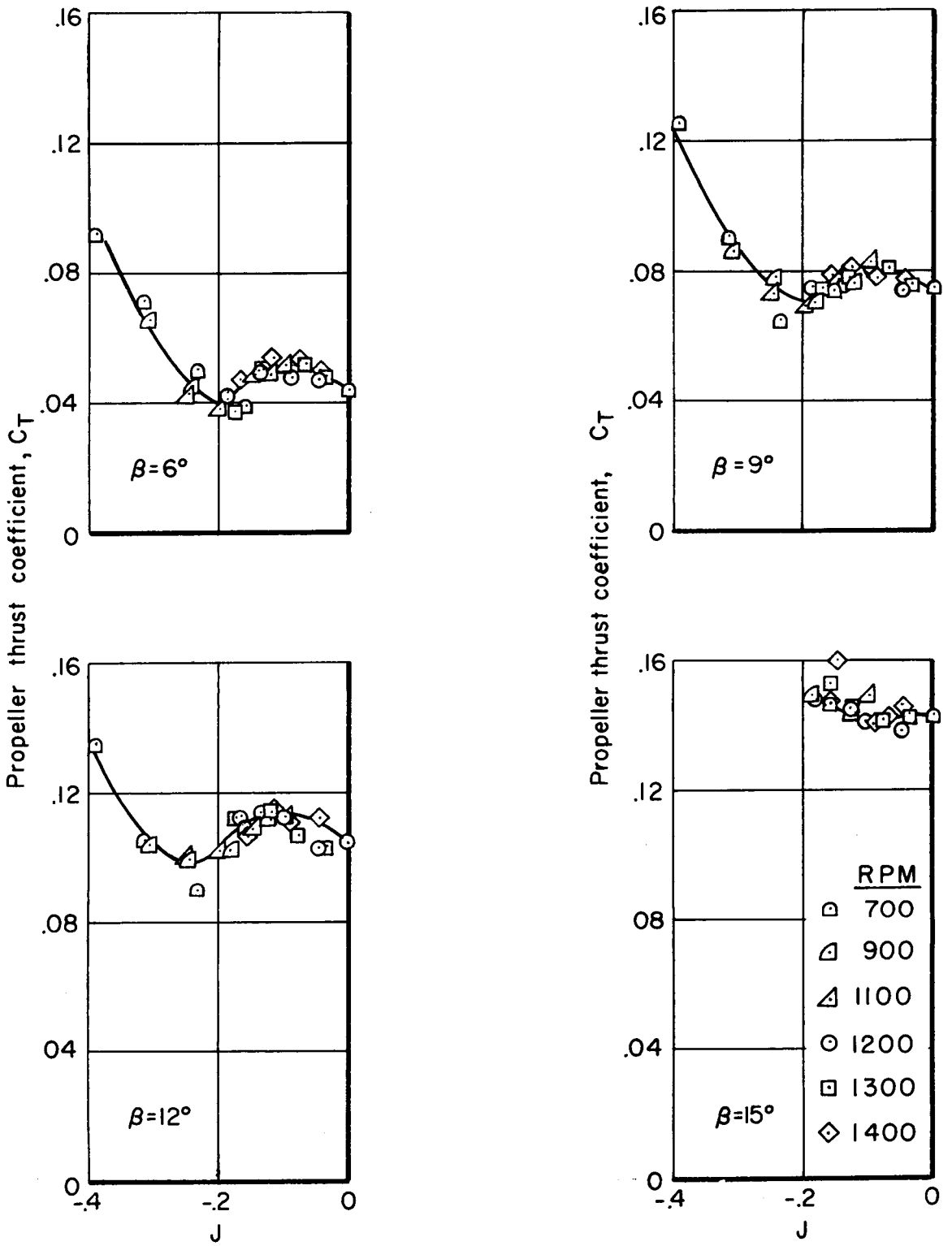

(b) $\alpha = 165^\circ$

Figure 3.- Continued.

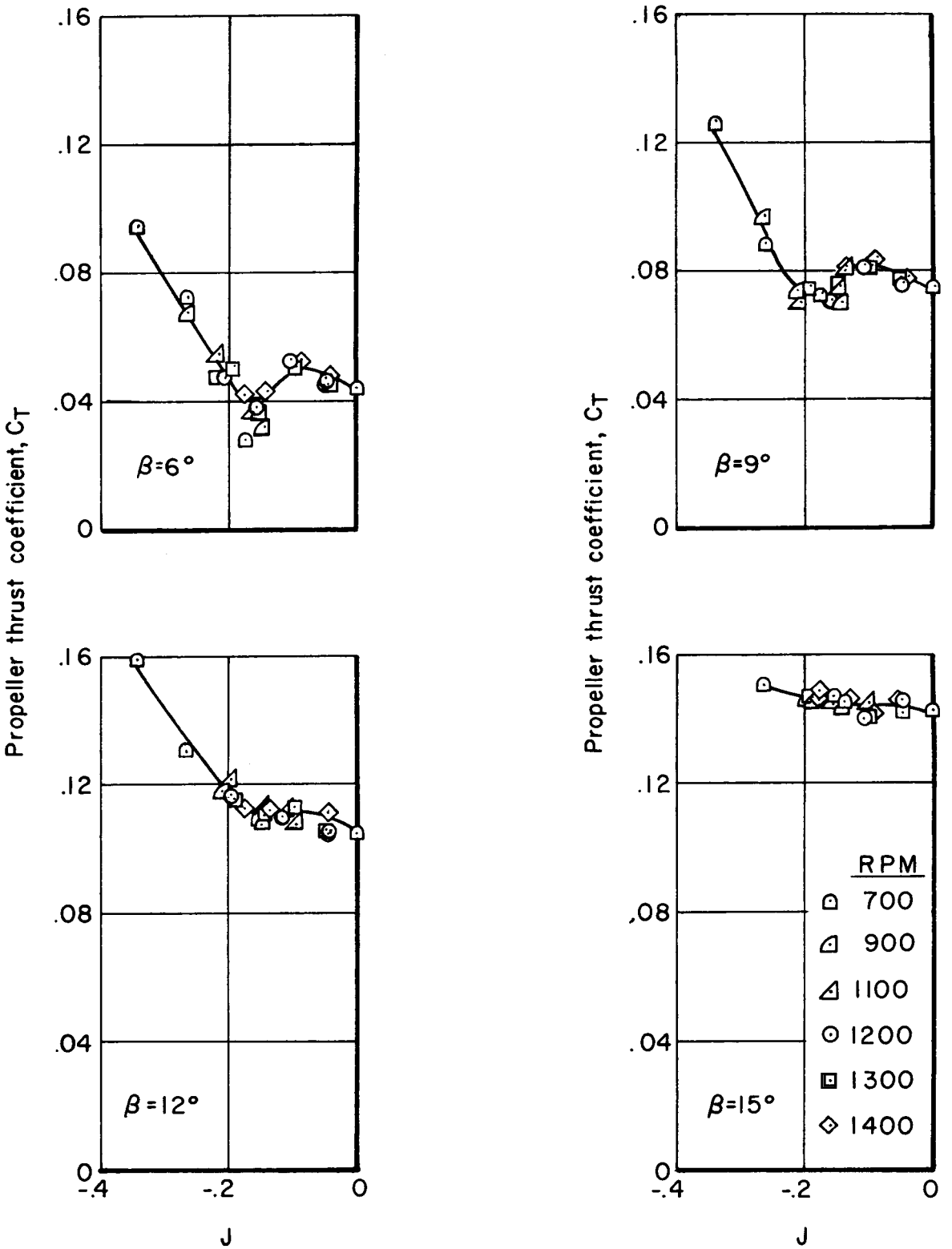

(c) $\alpha = 150^{\circ}$

Figure 3.- Continued.

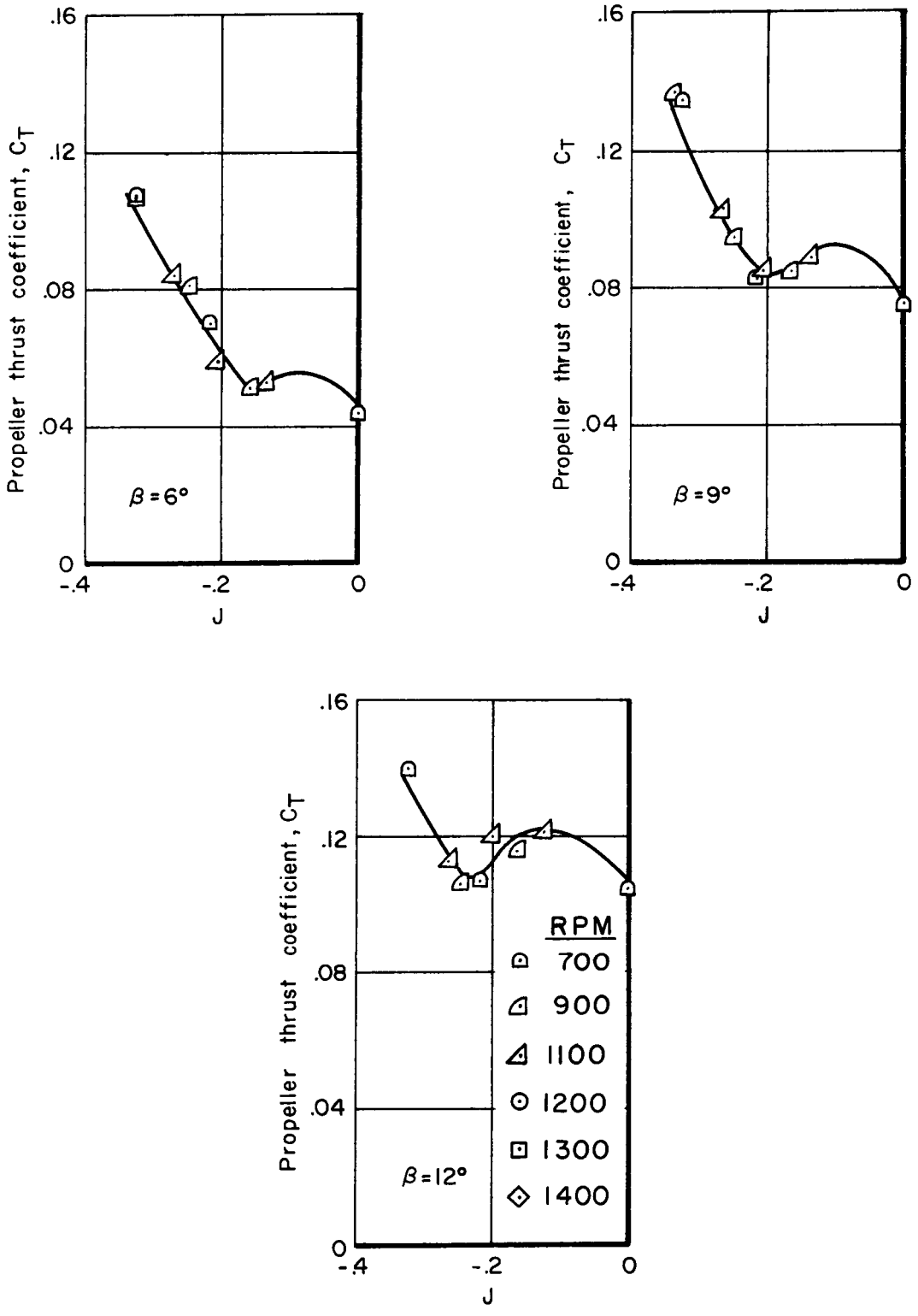

(d) $\alpha = 135°$

Figure 3.- Continued.

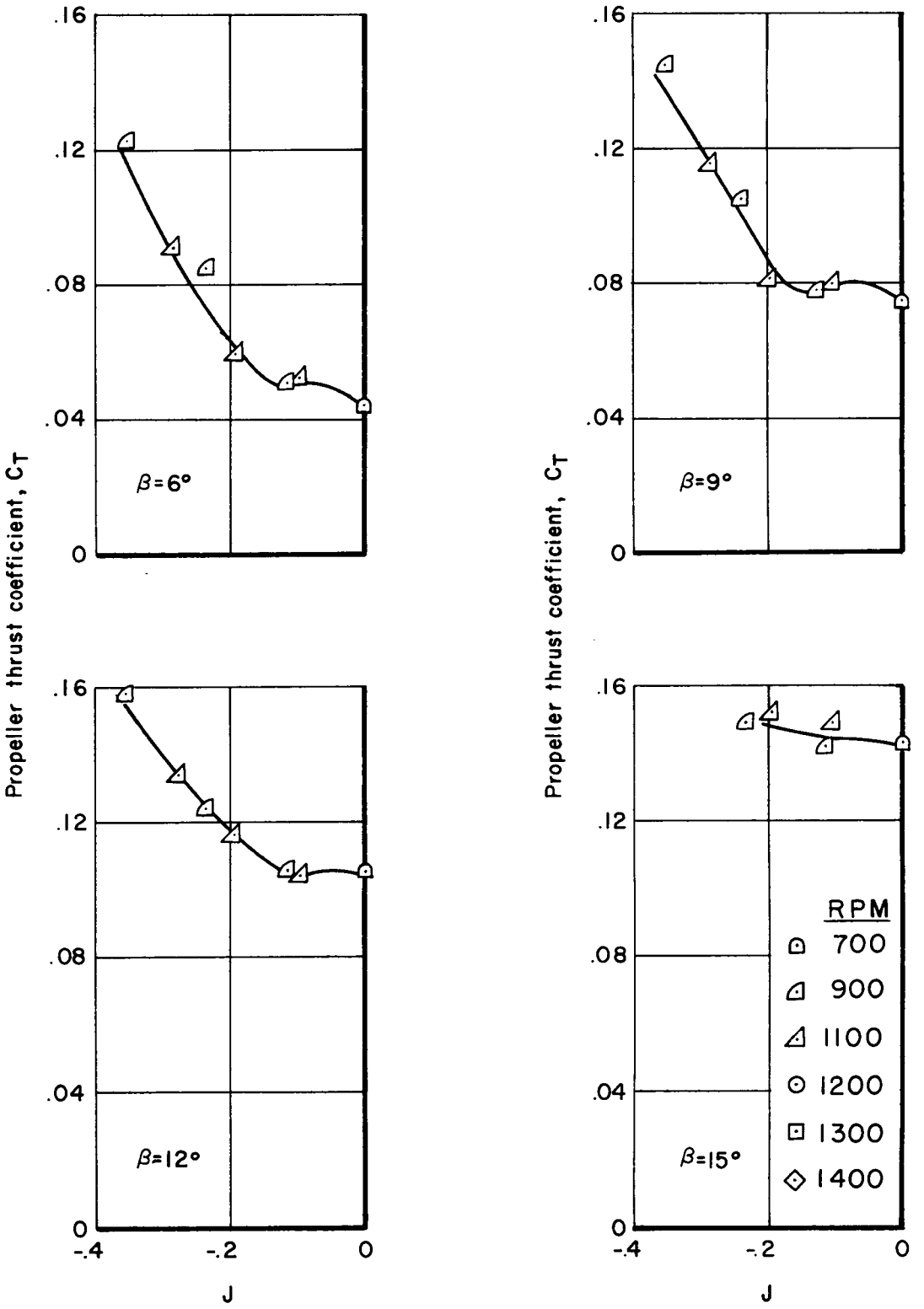

(e) $\alpha = 120^{\circ}$

Figure 3.- Concluded.

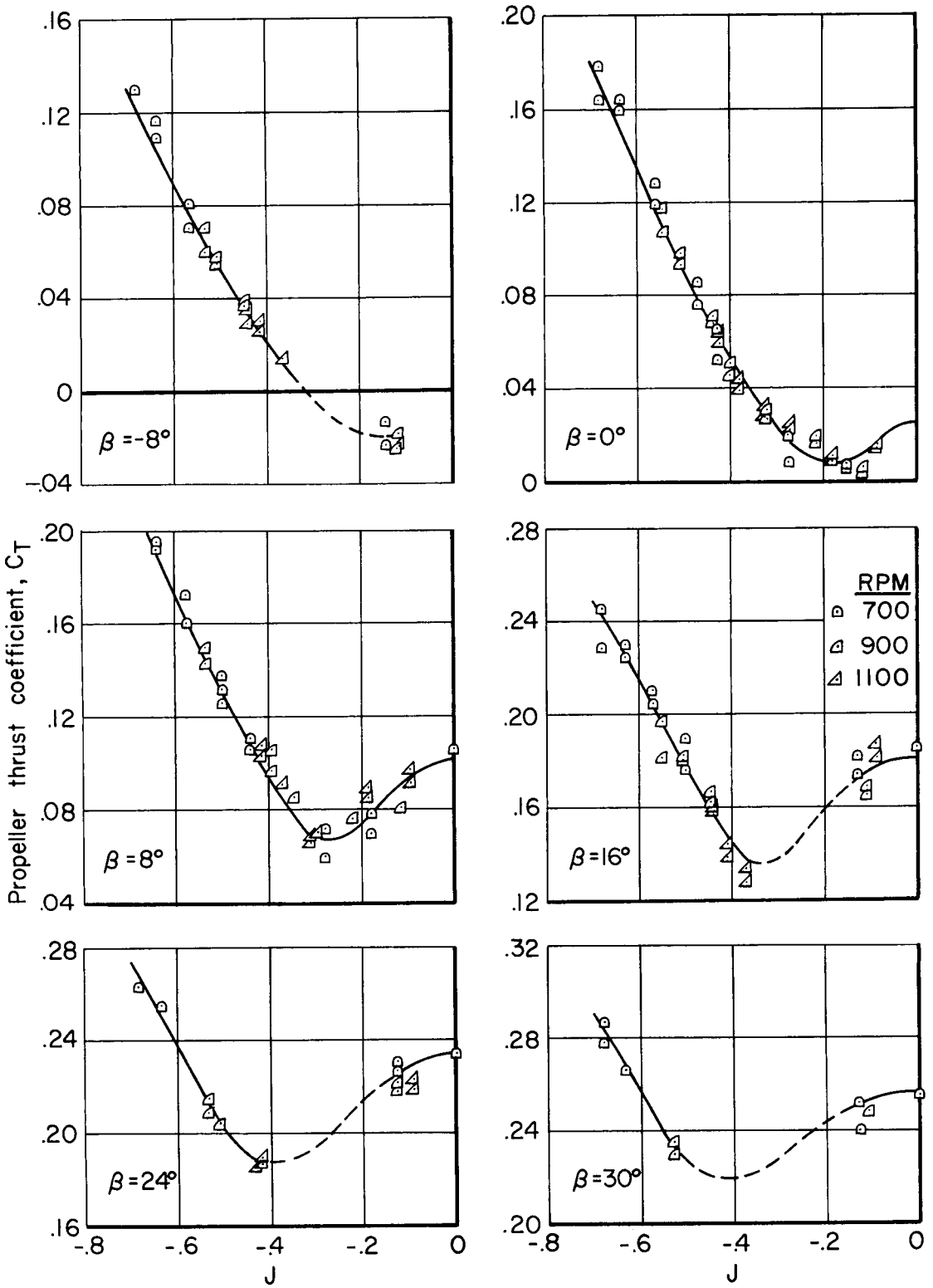

Figure 4.- Steady-state thrust coefficient as a function of propeller advance ratio for the rigid propeller; $\alpha = 180^{\circ}$.

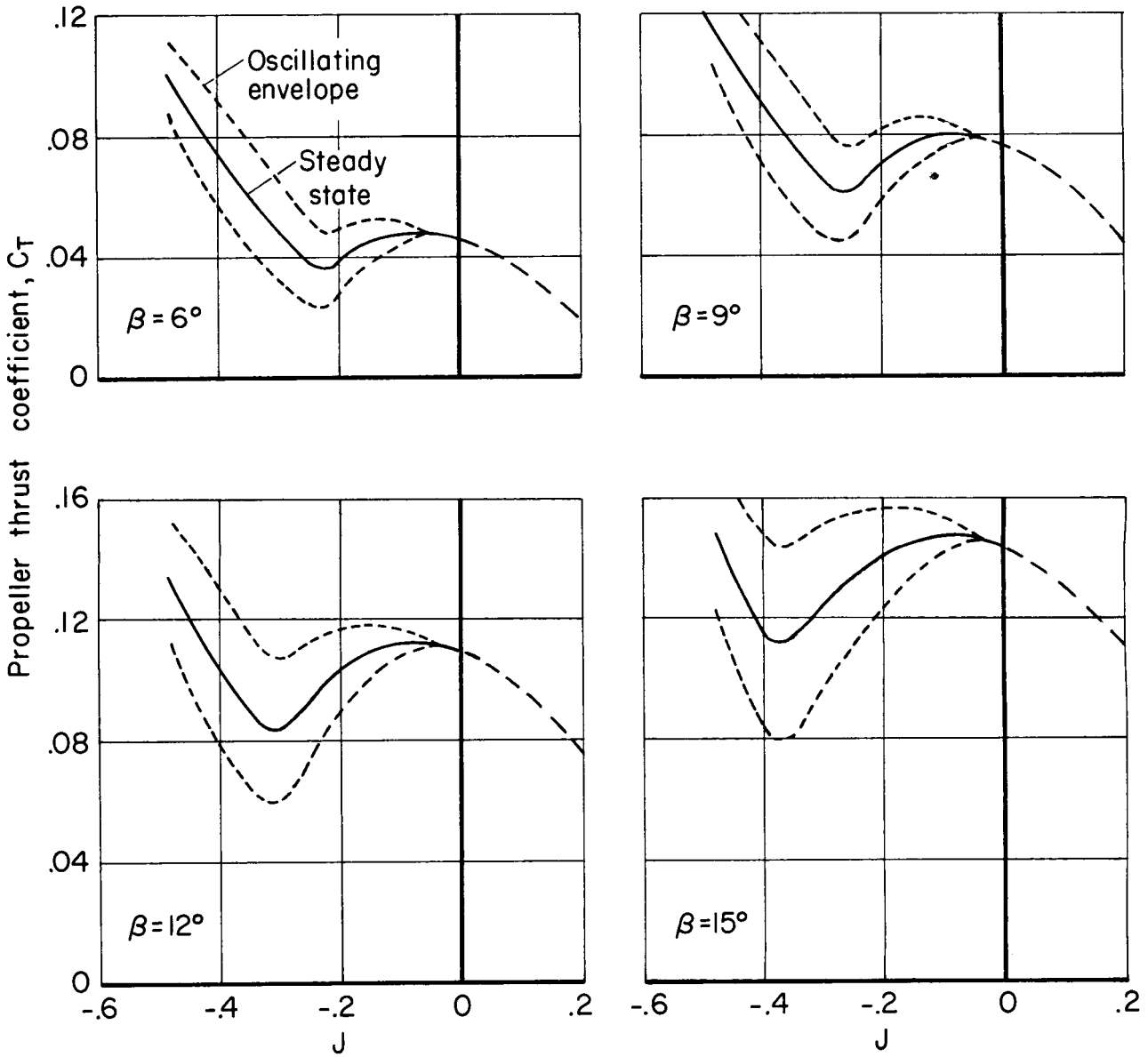

(a) $\alpha = 180^\circ$

Figure 5.- Steady-state and oscillating thrust coefficients as functions of propeller advance ratio for the flapping propeller.

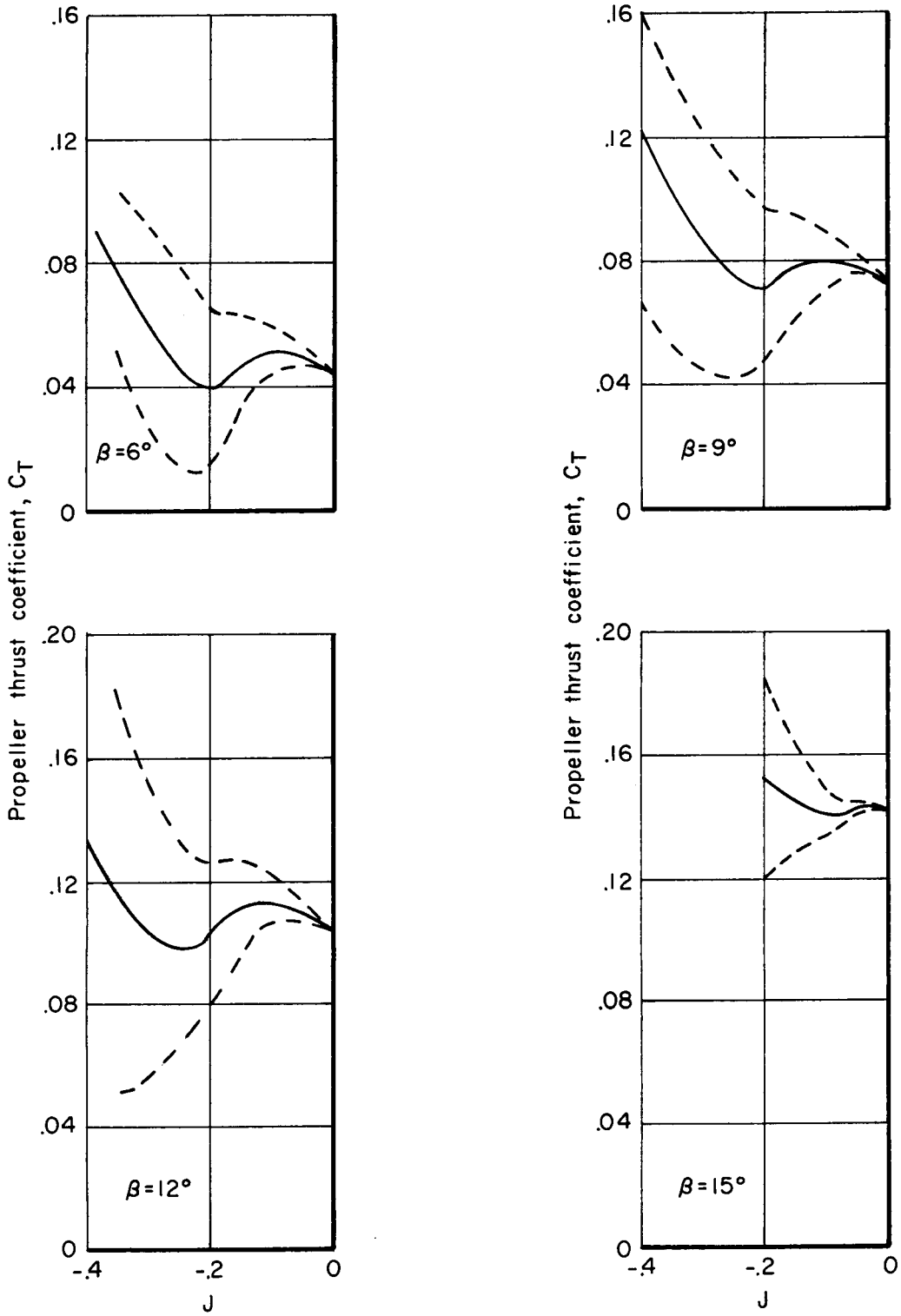

(b) $\alpha = 165°$

Figure 5.- Continued.

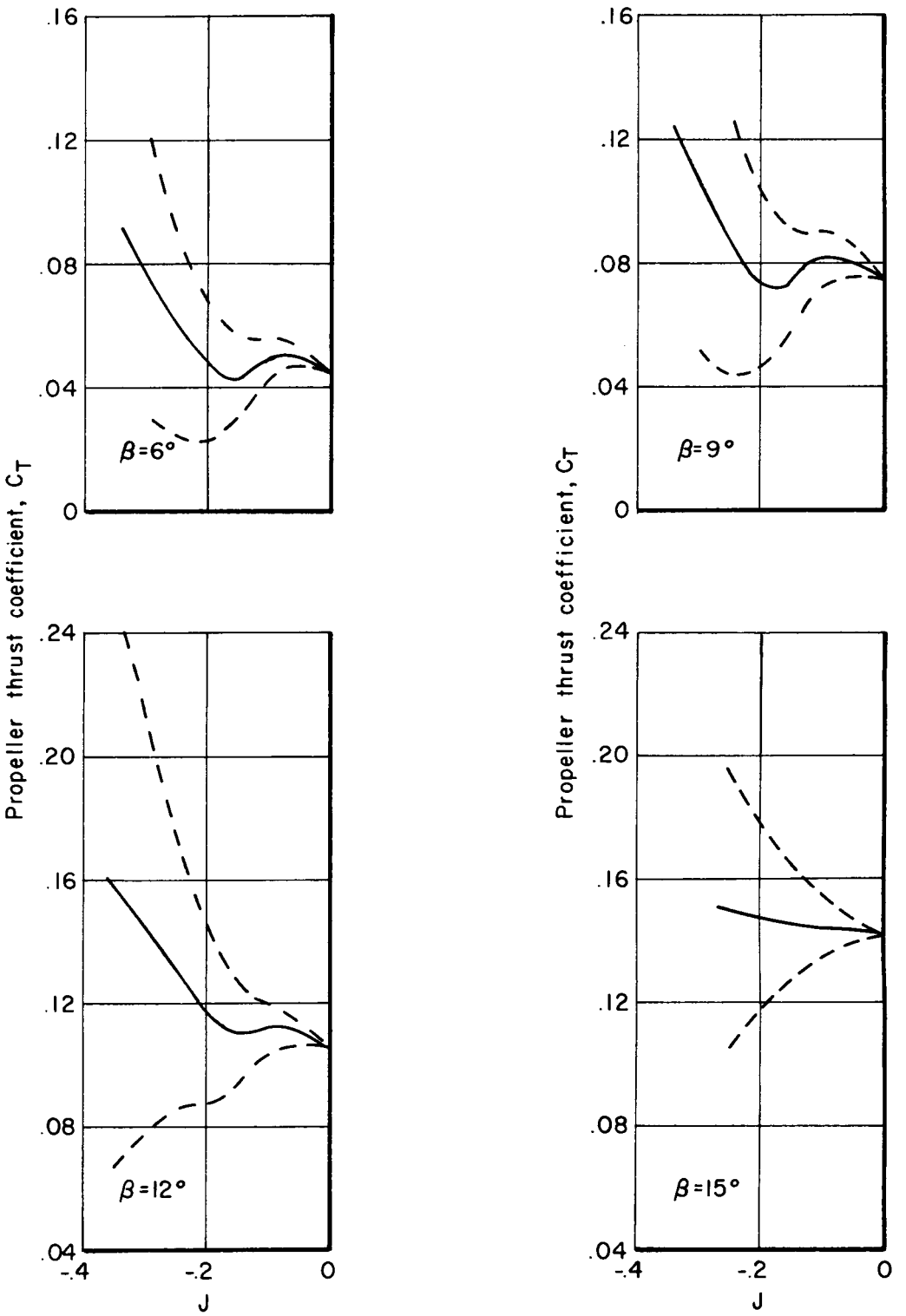

(c) $\alpha = 150^{\circ}$

Figure 5.- Continued.

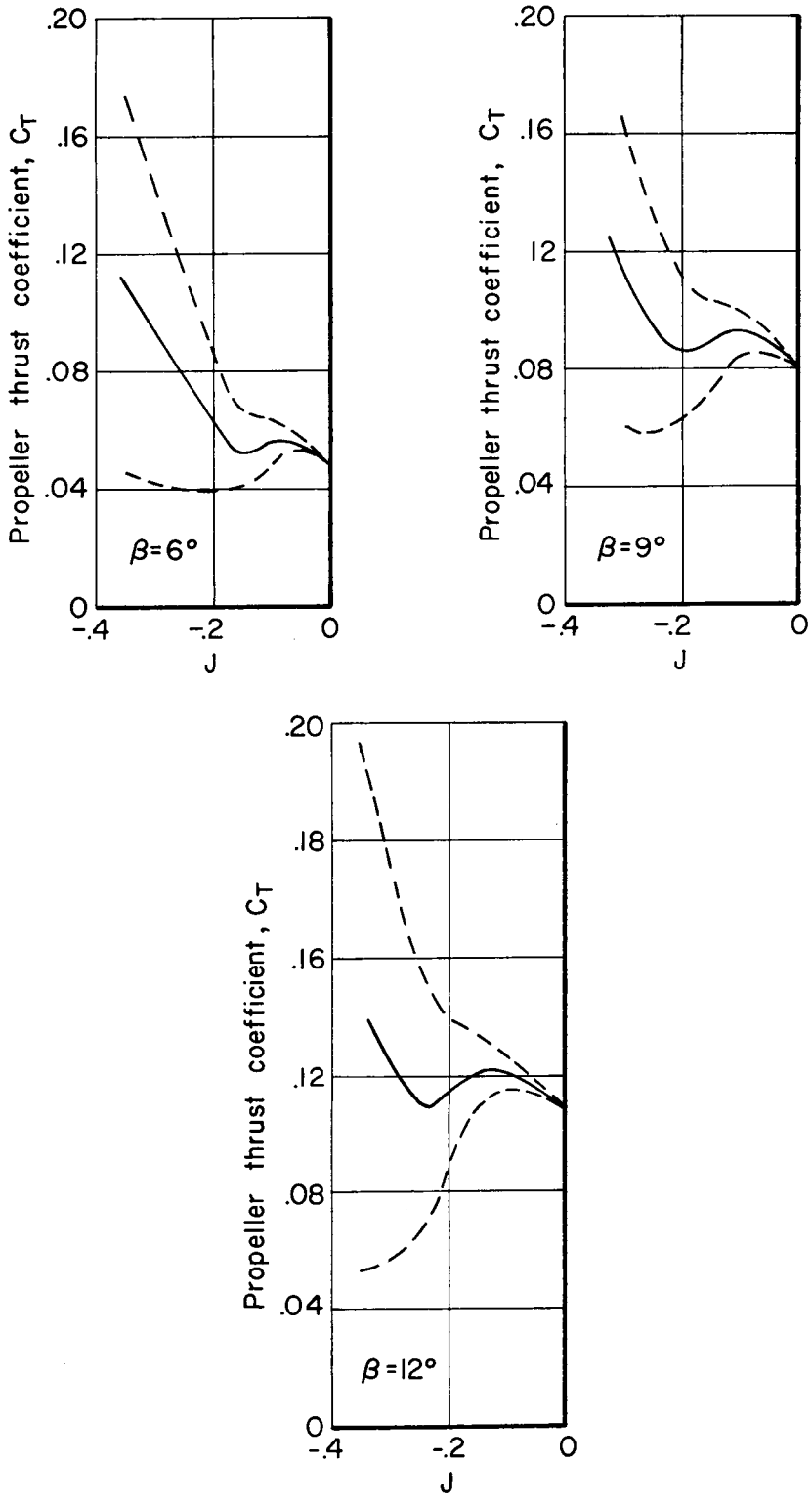

(d) $\alpha = 135^\circ$

Figure 5.- Continued.

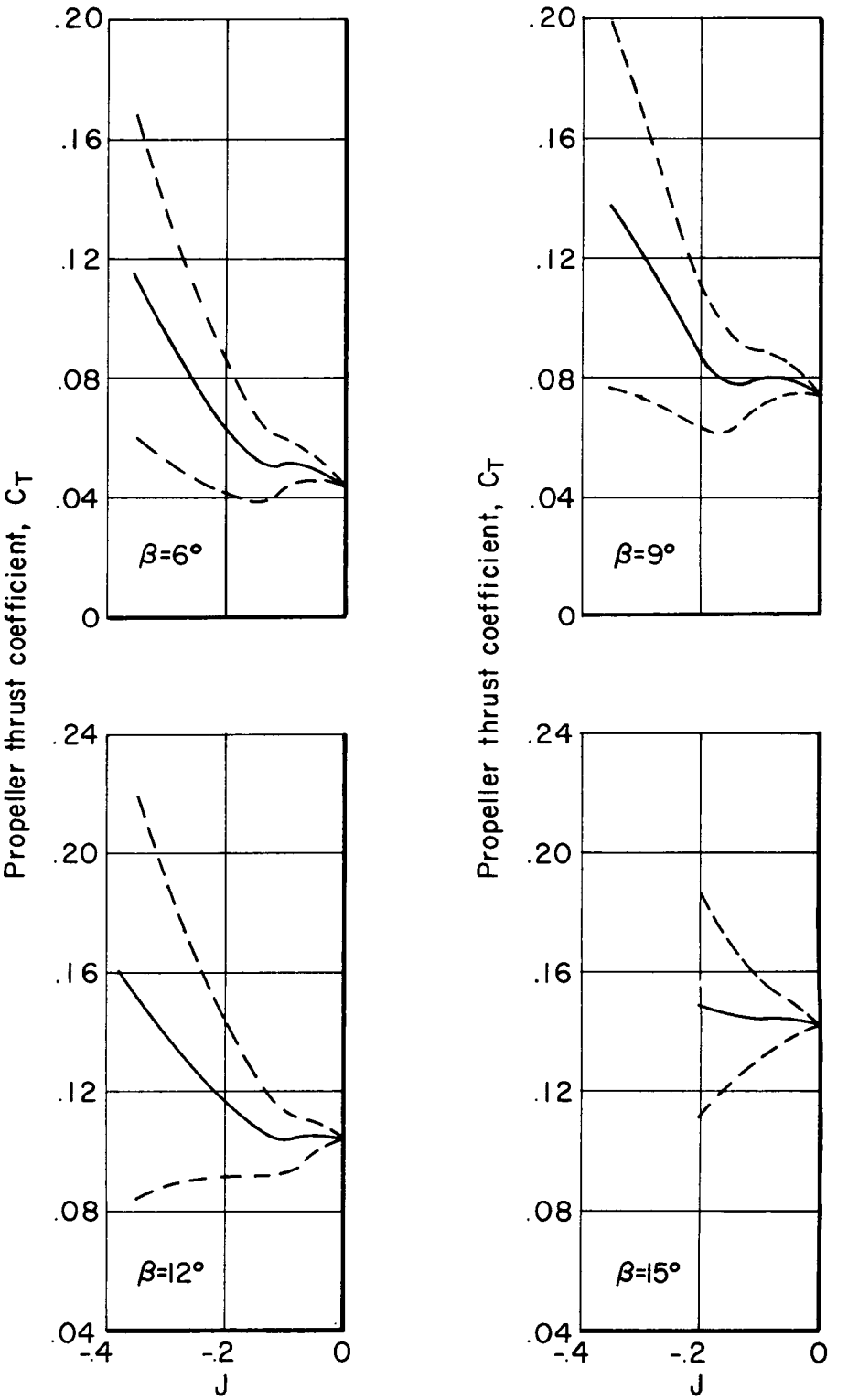

(e) $\alpha = 120^{\circ}$

Figure 5.- Concluded.

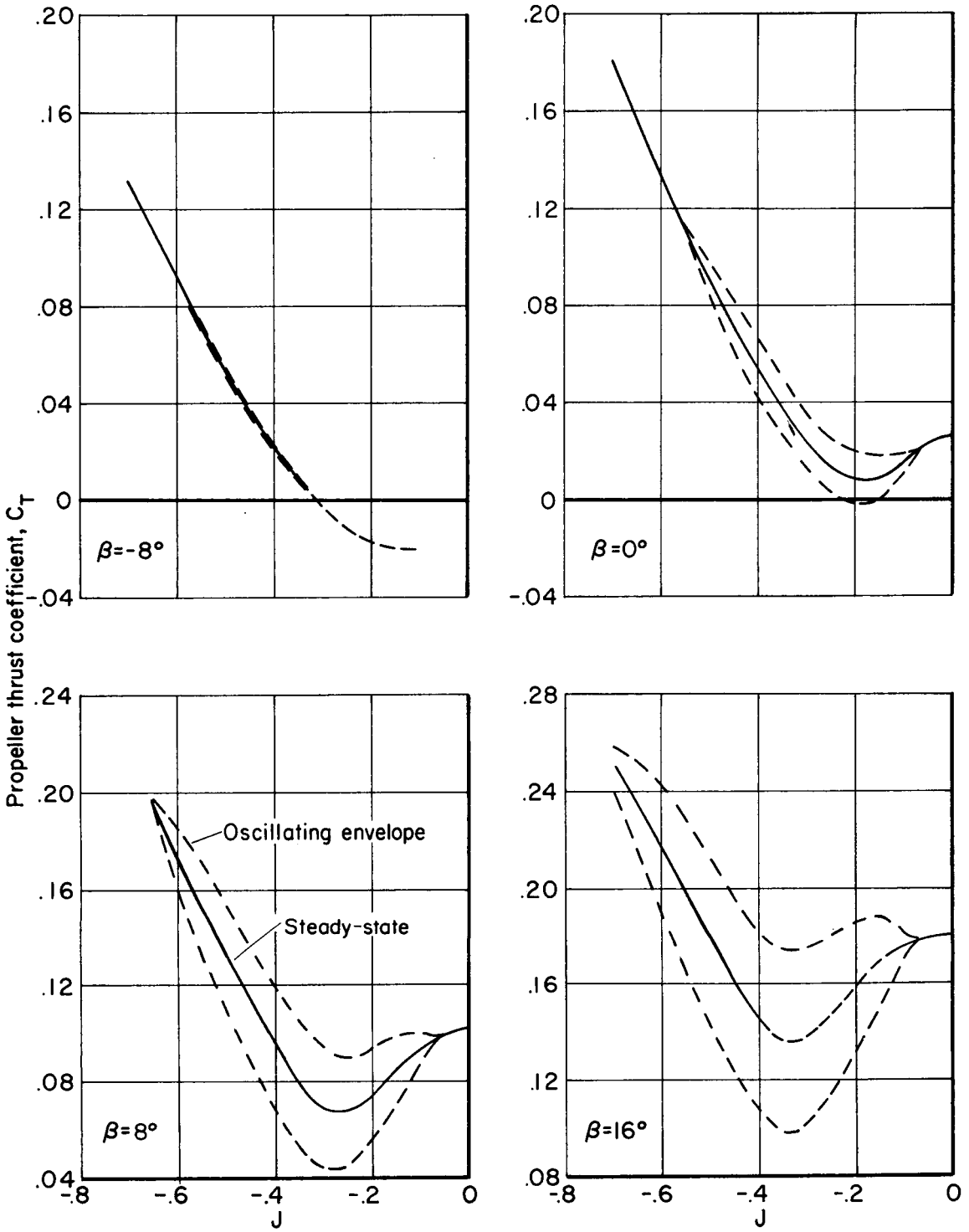

(a) β = -8° to +16°

Figure 6.- Steady-state and oscillating thrust coefficients as functions of propeller advance ratio for the rigid propeller; α = 180°.

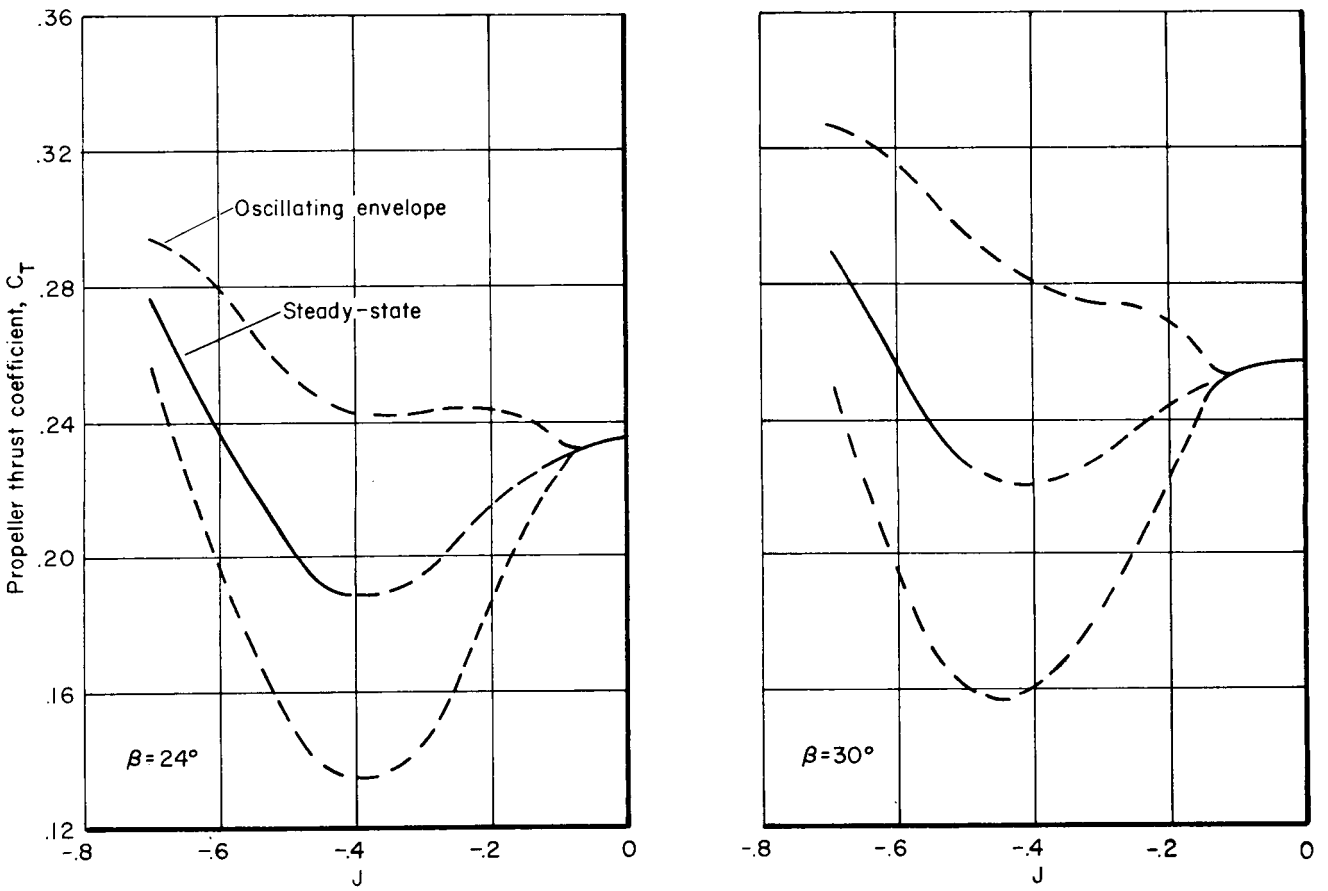

(b) $\beta = 24^{\circ}$ and 30°

Figure 6.- Concluded.

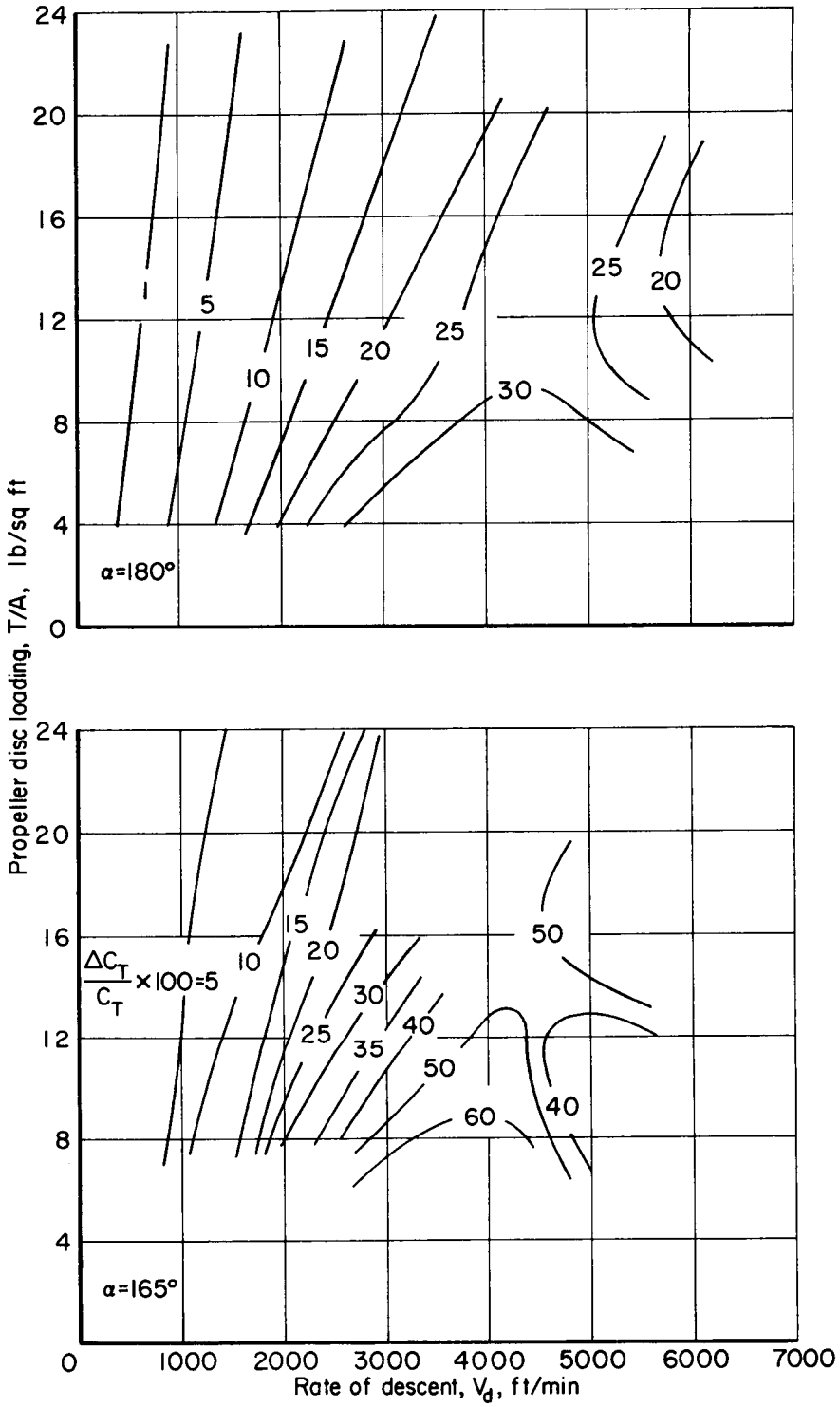

(a) α = 180° and 165°

Figure 7.- Thrust oscillation as a function of disc loading and rate of descent for the flapping propeller.

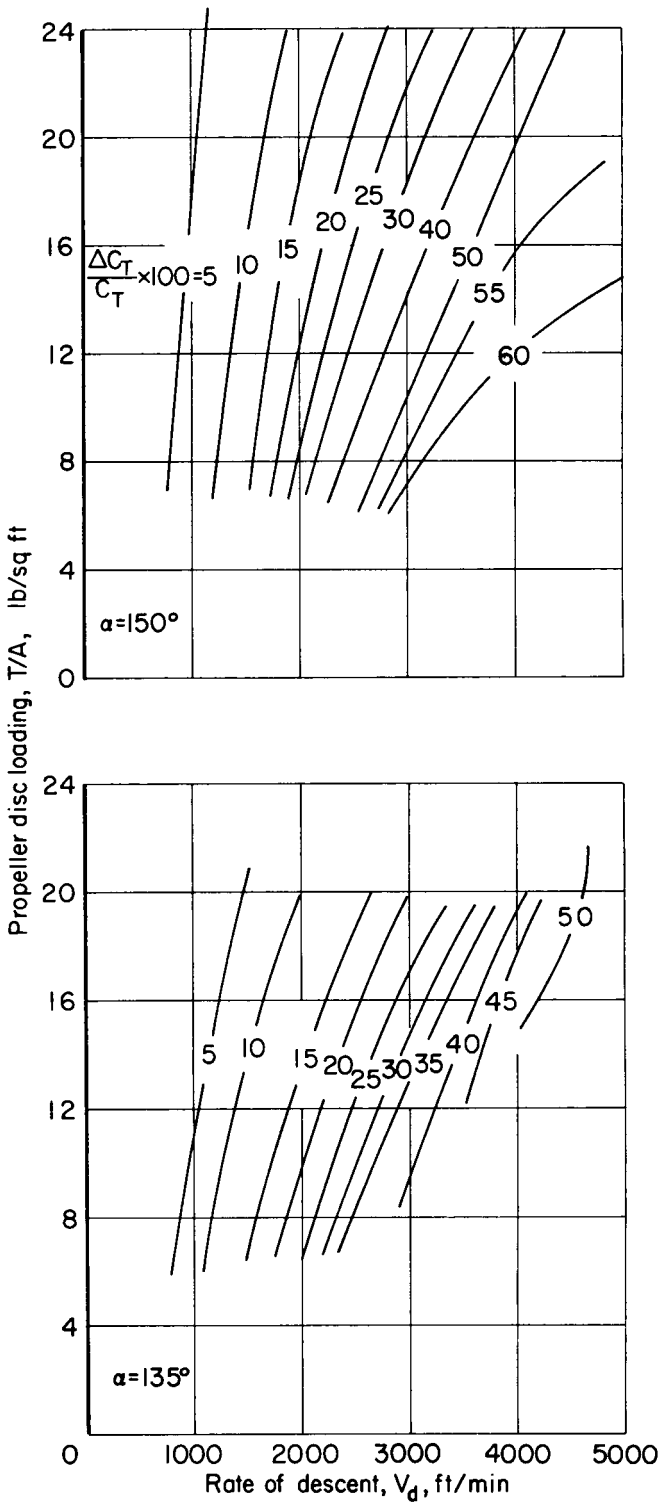

(b) $\alpha = 150^{\circ}$ and 135°

Figure 7.- Continued.

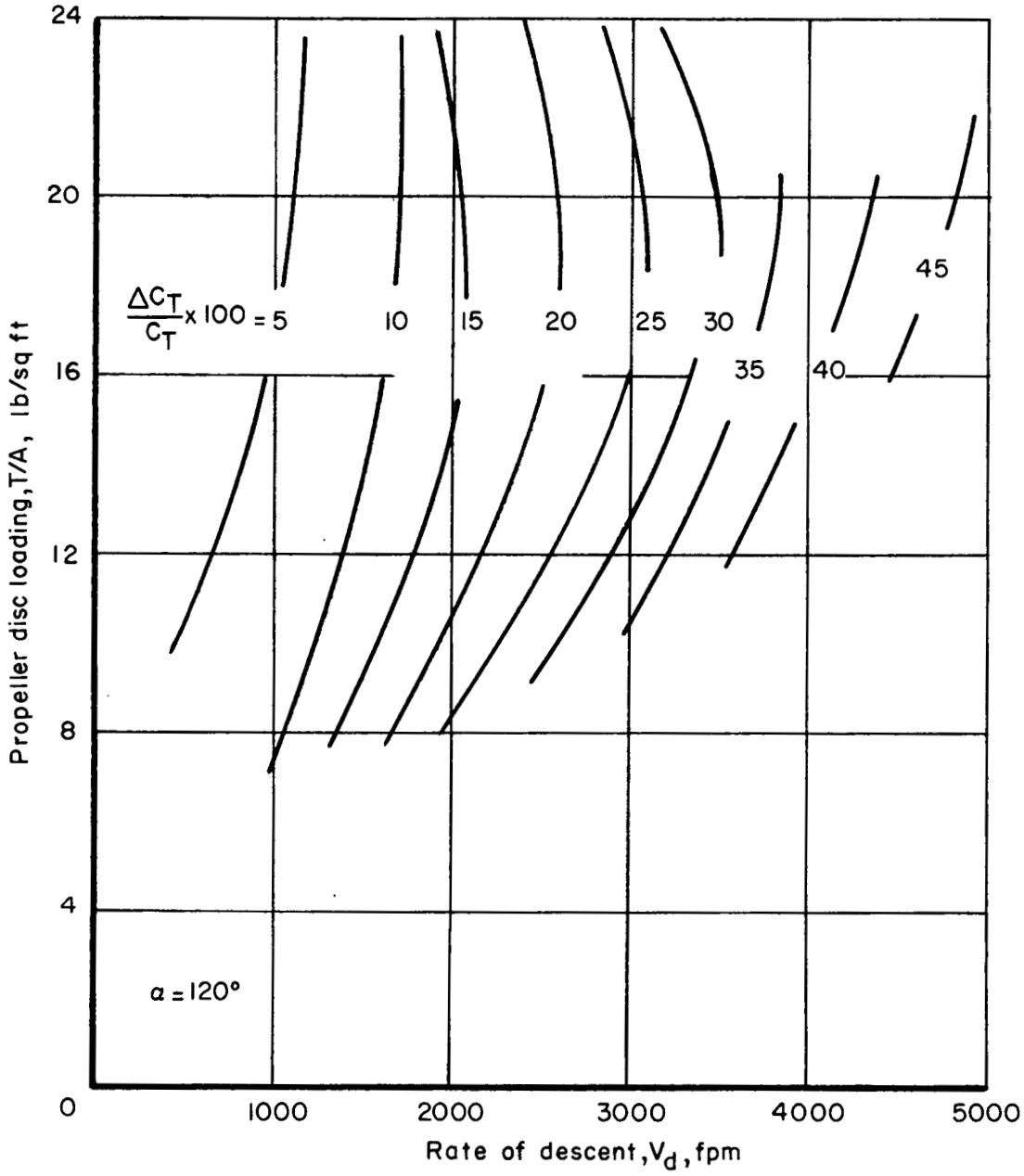

(c) $\alpha = 120^{\circ}$

Figure 7.- Concluded.

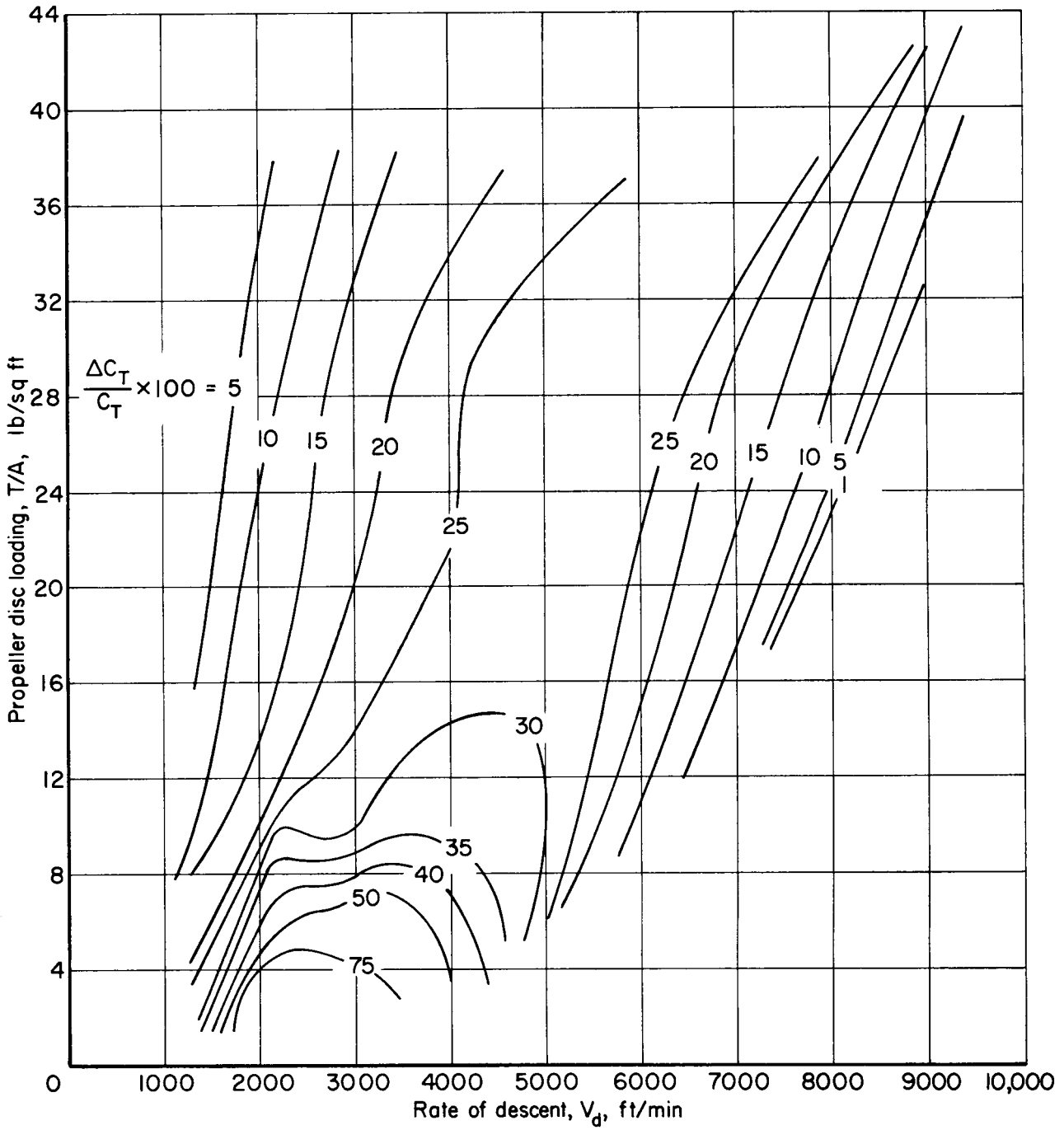

Figure 8.- Thrust oscillation as a function of disc loading and rate of descent for the rigid propeller; $\alpha = 180^{\circ}$.

NASA-Langley, 1963 A-625